Journal of Food and Drug Analysis

Volume 28 | Issue 1 Article 15

Involvement of prohibitin 1 and prohibitin 2 upregulation in cBSA-induced podocyte cytotoxicity

Recommended Citation

Wu, Heng-Hsiung; Chen, Chao-Jung; Lin, Pei-Yu; and Liu, Yu-Huei (2020) "Involvement of prohibitin 1 and prohibitin 2 upregulation in cBSA-induced podocyte cytotoxicity," *Journal of Food and Drug Analysis*: Vol. 28 : Iss. 1 , Article 15.
Available at: https://doi.org/10.1016/j.jfda.2019.09.003

Available online at www.sciencedirect.com

ScienceDirect

journal homepage: www.jfda-online.com

Original Article

Involvement of prohibitin 1 and prohibitin 2 upregulation in cBSA-induced podocyte cytotoxicity

Heng-Hsiung Wu [a], *Chao-Jung Chen* [b], *Pei-Yu Lin* [b,c], *Yu-Huei Liu* [b,c,*]

[a] *Graduate Institute of Biomedical Sciences, China Medical University, Taichung, Taiwan*
[b] *Graduate Institute of Integrated Medicine, China Medical University, Taichung, Taiwan*
[c] *Department of Medical Genetics and Medical Research, China Medical University Hospital, Taichung, Taiwan*

ARTICLE INFO

Article history:
Received 16 August 2019
Received in revised form
15 September 2019
Accepted 20 September 2019
Available online 18 October 2019

Keywords:
Membranous nephropathy
Prohibitin 1
Prohibitin 2

ABSTRACT

Membranous nephropathy (MN) is the most common cause of nephrotic syndrome in adults, when not effectively treated. The aim of this study was to discover new targets for the diagnosis and treatment of MN. A reliable mouse model of MN was used by the administration of cationic bovine serum albumin (cBSA). Mice with MN exhibited proteinuria, histopathological changes, and accumulation of immune complexes in the glomerular basement membrane. Label-free proteomics analysis was performed to identify changes in protein expression, and the overexpressed proteins were evaluated. There were 273 proteins that showed significantly different expression in mice with MN, as compared to the controls. String analysis showed that functions related to cellular catabolic processes were downregulated in MN. Among the differentially expressed proteins, prohibitin 1 (PHB1) and prohibitin 2 (PHB2) were upregulated in the kidneys of mice with MN, as demonstrated by immunohistochemistry (IHC), and this upregulation was observed in both the tubular cells and glomeruli. Both shRNA-mediated knockdown of PHB1 or PHB2 inhibited tumor suppressor p53 expression and significantly promoted podocyte proliferation. In addition, both PHB1 and PHB2 were responsible for cBSA-induced cytotoxicity. Microarray analysis further revealed that the upregulation of PHB1 and PHB2 may be due to a blockage of proteasome activity. These data demonstrate that the upregulation of PHB2 is involved in cBSA-mediated podocyte cytotoxicity, which may lead to MN development.

1. Introduction

The incidence of chronic kidney disease (CKD) in Taiwan is increasing. According to the latest 2018 record, the prevalence rate has increased to 2599 individuals per million population. Both the incidence and prevalence of CKD in Taiwan are the highest rates in the world. In addition, the number of people on dialysis in Taiwan has reached 85,000, and the dialysis rate

* *Corresponding author*. Graduate Institute of Integrated Medicine, China Medical University, Taichung, Taiwan. Fax: +886 4 22033295. E-mail address: yuhueiliu@mail.cmu.edu.tw (Y.-H. Liu).
https://doi.org/10.1016/j.jfda.2019.09.003

is the highest in the world. The relationship between CKD and renal cancer in Taiwan was evaluated [1], and the results suggest that more attention should be given to the risk of cancer for CKD patients.

Membranous nephropathy (MN), while rare in children, is the most common cause of nephrotic syndrome in male adults, and is considered to be an autoimmune disease [2,3]. Nephrotic syndrome caused by MN results in significant proteinuria, hypoalbuminemia, and edema. Both genetic and environmental factors may contribute to the development of MN. The most well-characterized autoantibodies produced in MN are a result of genetic abnormality and recognize targets on the podocyte slit, including: (1) anti-neutral endopeptidase (NEP) autoantibody, resulting from alloimmunization [4]; (2) anti-phospholipase A2 receptor 1 (PLA2R1) autoantibody, which is found in about 70–80% of patients with recurrent MN after renal transplantation [5] and which is associated with disease remission and progression [6–8], but does not express in mice; and (3) anti-thrombospondin type 1 domain-containing 7 A (THSD7A) autoantibody, which is found in about 2–3% of patients with primary MN [9–12]. However, there are currently no drugs targeting on these that target these autoantibodies, in part due to the lack of a specific animal model for genetical MN [9].

Anti–bovine serum albumin antibodies targeting a modified food antigen, cationic bovine serum albumin (cBSA), which appears to become seeded in the anionic glomerular capillary wall where it induces the formation of immune complexes, is found in about 2% of patients, mainly children. MN mice induced with repeated doses of cBSA is an established mouse model to aid in better understanding disease progression [3,13–15]. Indeed, several studies have indicated the importance of podocyte in protecting against complement activation and the effects of prolonged ER stress. However, the current drugs used for the treatment of MN include angiotensin-converting enzyme (ACE) inhibitors, angiotensin II receptor blockers (ARBs), diuretics, and immunosuppressants, may increase the risk of infection and cause other adverse effects. In addition, about 30% of patients diagnosed with MN eventually progress to renal failure, although renal transplant can be a treatment option. Further understanding of the pathogenesis of MN will provide new opportunities for the development of a therapeutic strategy for MN, which will aid in delaying disease progression.

Label-free quantitative proteomic technique is an important technique in basic and applied biomedical research, due to its efficiency in analyzing large-scale protein expression simultaneously to evaluate the complex molecular basis of a pathological process. Here, we used label-free quantitative proteomics to compare altered global protein expression between kidney tissues of cBSA-induced MN mice and those of controls. The mechanisms of upregulation of two mitochondrial proteins, PHB1 and PHB2, were examined for cBSA-induced kidney damage.

2. Methods

2.1. *Mouse MN model*

All animal experiments were performed according to regulations approved by the Laboratory Animal Center, China Medical University, 100-58-N. BALB/c mice (male, 4–6 weeks old) were obtained from Bio-LASCO Taiwan. The mice were kept in the Laboratory Animal Center of China Medical University under specific-pathogen-free conditions. The mice were divided into two groups, MN and control (n = 5 each group). The experimental mice were immunized with 1 mg of cationic bovine serum albumin (cBSA, #9058, Chondrex) and Freund's complete adjuvant (#7008, Chondrex). Two weeks later, the mice were further injected with 3 mg/kg of cBSA intravenously thrice weekly on every alternate day for 4 weeks. Proteinuria was measured as the ratio of urinary protein (mg/mL) to urinary creatinine (mg/dL) (Up/Ucr).

2.2. *Histopathological analysis*

The kidney tissues were fixed in formaldehyde and were then embedded in paraffin. The tissue sections (5 mm-thickness) were stained with hematoxylin and eosin (H&E), Periodic Acid-Schiff (PAS), or Masson's Trichrome staining. The slides were scanned using Pannoramic Digital Slide Scanners and observed using digital CaseViewer 2.2 (3DHISTECH).

2.3. *Label-free quantitative proteomics*

Label-free quantitative proteomics was performed using nanoLC-MS/MS analysis, as described previously [16]. The protein extracts from kidney tissues were quantified in each group (n = 3 in each group). Equal amounts of kidney protein extracts from each mouse were obtained for analyses. The trypsin-digested peptide samples were injected into a trap column (C18, 5 mm, 100 Å) with a flow rate of 10 mL/min for a duration of 5 min. The trapped analyses were then separated by an analytical column (Acclaim PepMap C18, 2 μm 100 Å, 75 μm × 250 mm, Thermo Scientific, USA) with a flow rate of 300 nL/min. An acetonitrile/water gradient of 1%–35% for 120 min was used for peptide separation. For MS/MS detection, peptides with charge 2+, 3 + or 4 + were selected for data-dependent acquisition, which was set to one full MS scan with 1 Hz, and switched to ten product ion scans with 10 Hz. The LC-MS/MS spectra were converted to xml files using DataAnalysis (version 4.1, Bruker). The xml files were searched against the Swissport (release 51.0) database using the MASCOT search algorithm (version 2.2.07). The search parameters for MASCOT for peptide and MS/MS mass tolerance were 70 ppm and 0.06 Da, respectively. Search parameters were selected as Taxonomy – mus; enzyme – trypsin; fixed modifications – carbamidomethyl (C); variable modifications – oxidation (M). Peptides were considered as identified when their MASCOT individual ion score was higher than 25. Label-free quantitative proteomics was achieved by LC-MS replicated runs (n = 2) of different groups. LC-MS/MS runs of each group were performed for protein identification. Molecular features were produced from LC-MS results with DataAnalysis 4.1 (Bruker Daltonics). ProfileAnalysis (version 2.0, Bruker Daltonics) was used to process molecular features for *t*-test comparison between two groups. The comparison results of molecular features were transferred to ProteinScape 3.1 (Bruker Daltonics) and integrated with protein identification results to obtain quantified peptide information of each protein.

2.4. *Immunohistochemical (IHC) staining*

The slides were deparaffinized and hydrated, and antigens were retrieved and heated in a microwave, followed by incubation with goat anti-mouse IgG (Jackson ImmunoResearch), anti-PHB1 (GTX101105, GeneTex), and anti-PHB2 (GTX102100, GeneTex) antibodies overnight at 4 °C. The slides were then incubated with Horseradish peroxidase-conjugated anti-rabbit secondary antibody (Jackson ImmunoResearch) against PHB1 and PHB2 for 1 h at around 25 °C. The reactions were visualized using a 3,3′-diaminobenzidine (DAB) kit substrate solution (DAKO) for 2–3 min, followed by counterstaining with hematoxylin. The slides were scanned using Pannoramic Digital Slide Scanners and observed using digital CaseViewer 2.2 (3DHISTECH).

2.5. *Cell culture*

The human primary podocytes were obtained from Celprogen (Torrance) and culture media was purchased from Thermo Fisher Scientific (Waltham). The human primary podocytes were maintained in Roswell Park Memorial Institute 1640 medium (31800-022) with 10% fetal bovine serum, 50 U/mL penicillin and 50 μg/mL streptomycin, at 37 °C in a humidified atmosphere of 5% CO_2.

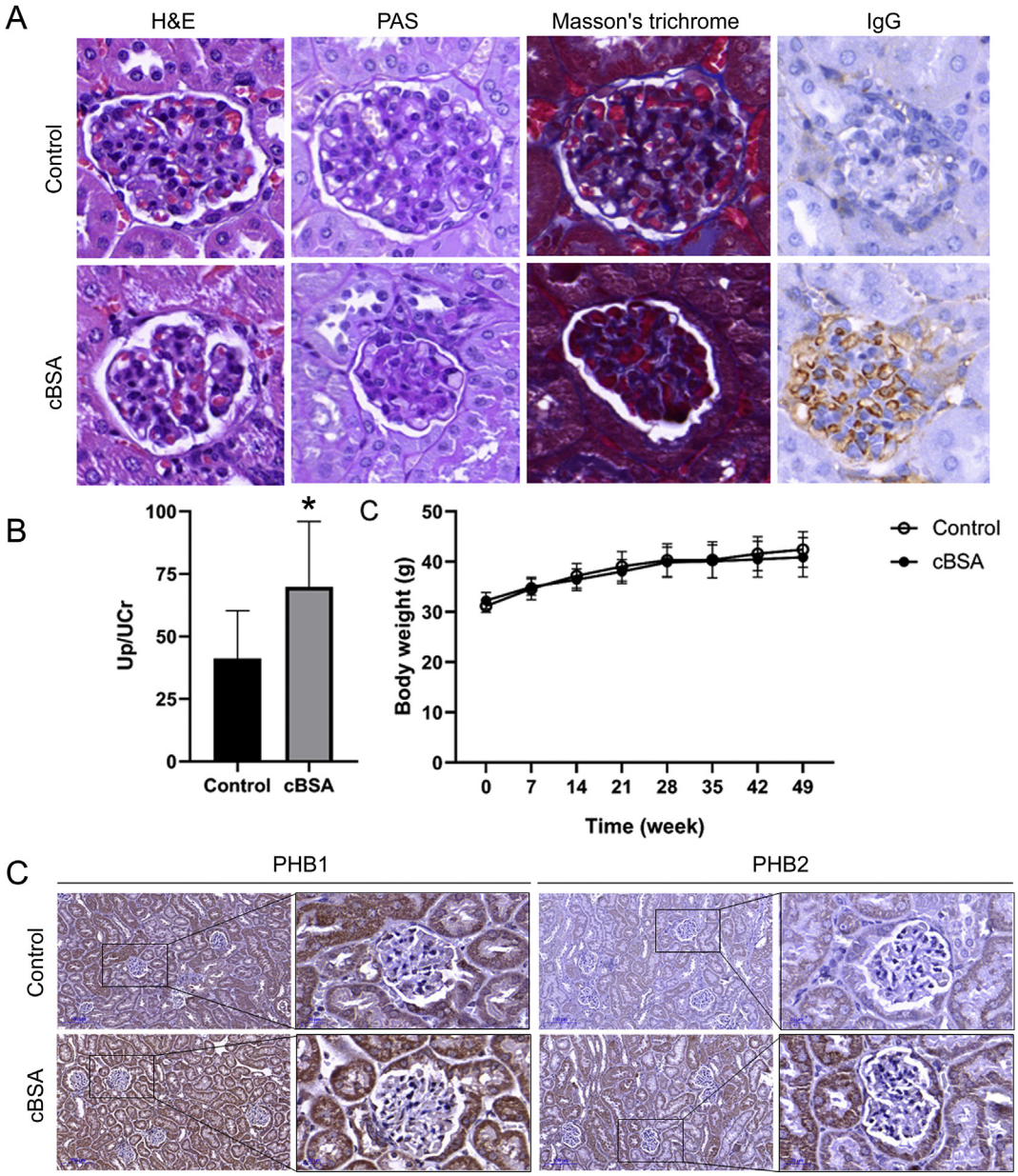

Fig. 1 – Histopathological and biochemical characteristics in mice with MN. (A) Mice with MN show a diffuse thickening of the glomerular capillary walls and diffuse subepithelial fibrinoid deposits, which are PAS-positive and shown in red due to staining with Masson's trichrome. Granular deposits of IgG along the glomerular basement membrane were also seen. (B) Mice with MN show overt proteinuria, as demonstrated by high Up/Ucr. (C) Mice with MN show similar body weight compared to controls. *P < 0.05. (D) Representative images of PHB1 and PHB2 stained by immunohistochemistry (IHC) in kidney tissues from mice with or without MN. Scale bar, 100 μm. High power field (HPF): 40× magnification.

Table 1 – Top 20 up-/down-regulated proteins changing in response to MN development. Protein common name and description are listed. Complete dataset was shown in supplementary table 1.

Protein name	Description	Mw [kDa]	pI	Experiment A			Experiment B		
				Scores	SC [%]	Ratio of MN/Control	Scores	SC [%]	Ratio of MN/Control
Upregulation									
PSB4	Proteasome subunit beta type-4	29.1	5.3	336.6 (M:336.6)	32.2	2.90	247.7 (M:247.7)	23.9	4.00
PHB2	Prohibitin-2	33.3	10.2	936.6 (M:936.6)	55.2	3.78	882.3 (M:882.3)	50.8	3.79
SSRD	Translocon-associated protein subunit delta	18.9	5.4	316.2 (M:316.2)	53.5	3.78	376.3 (M:376.3)	53.5	3.60
RAB7A	Ras-related protein Rab-7a	23.5	7.2	561.1 (M:561.1)	64.3	2.90	566.4 (M:566.4)	56.5	3.27
SMD1	Small nuclear ribonucleoprotein Sm D1	13.3	12.1	70.9 (M:70.9)	16.8	2.02	62.6 (M:62.6)	16.8	3.27
ATPB	ATP synthase subunit beta, mitochondrial	56.3	5.1	3791.4 (M:3791.4)	80.2	3.00	3630.6 (M:3630.6)	74.7	3.13
CRYAB	Alpha-crystallin B chain	20.1	6.9	584.0 (M:584.0)	80.6	4.83	529.3 (M:529.3)	82.9	2.88
FABP3	Fatty acid-binding protein, heart	14.8	6.1	468.0 (M:468.0)	47.4	3.00	481.2 (M:481.2)	42.1	2.88
GAPDH	Glyceraldehyde-3-phosphate dehydrogenase	35.8	9.2	1339.9 (M:1339.9)	54.4	2.02	1331.5 (M:1331.5)	54.4	2.88
GSTT2	Glutathione S-transferase theta-2	27.6	7.8	325.9 (M:325.9)	32.4	2.90	230.6 (M:230.6)	15.6	2.88
AT5F1	ATP synthase subunit b, mitochondrial	28.9	9.6	698.3 (M:698.3)	39.5	2.64	605.3 (M:605.3)	37.5	2.67
CK054	Ester hydrolase C11orf54 homolog	35.0	5.8	118.8 (M:118.8)	21.3	1.64	113.5 (M:113.5)	14.3	2.67
MPV17	Protein Mpv17	19.7	10.2	118.4 (M:118.4)	13.1	2.42	136.4 (M:136.4)	13.1	2.67
PHB	Prohibitin	29.8	5.5	1111.1 (M:1111.1)	77.9	2.72	941.5 (M:941.5)	74.6	2.67
PGK1	Phosphoglycerate kinase 1	44.5	9.0	542.8 (M:542.8)	32.1	2.12	352.1 (M:352.1)	19.4	2.57
AK1CL	Aldo-keto reductase family 1 member C21	36.9	6.9	117.2 (M:117.2)	9.9	1.61	107.5 (M:107.5)	9.9	2.48
LGUL	Lactoylglutathione lyase	20.8	5.1	520.6 (M:520.6)	66.8	2.29	647.3 (M:647.3)	70.7	2.48
MPC2	Mitochondrial pyruvate carrier 2	14.3	11.3	165.5 (M:165.5)	31.5	2.29	104.8 (M:104.8)	17.3	2.48
ODB2	Lipoamide acyltransferase component of branched-chain alpha-keto acid dehydrogenase complex, mitochondrial	53.2	9.5	85.6 (M:85.6)	5.2	2.49	73.2 (M:73.2)	2.9	2.48
SUCB2	Succinyl-CoA ligase [GDP-forming] subunit beta, mitochondrial	46.8	6.7	444.4 (M:444.4)	25.6	2.42	535.1 (M:535.1)	30.0	2.48
Downregulation									
APOH	Beta-2-glycoprotein 1	38.6	9.7	802.2 (M:802.2)	46.4	0.34	591.0 (M:591.0)	40.9	0.26
ALBU	Serum albumin	68.6	5.7	2974.7 (M:2974.7)	67.4	0.25	3215.8 (M:3215.8)	68.8	0.25
CALM	Calmodulin	16.8	3.9	832.0 (M:832.0)	71.8	0.19	1106.4 (M:1106.4)	71.8	0.24
AMRP	Alpha-2-macroglobulin receptor-associated protein	42.2	7.9	155.9 (M:155.9)	9.7	0.22	184.2 (M:184.2)	7.2	0.24
CAH2	Carbonic anhydrase 2	29.0	6.5	199.6 (M:199.6)	22.7	0.18	306.5 (M:306.5)	32.3	0.23
SET	Protein SET	33.4	4.1	149.0 (M:149.0)	12.8	0.24	200.8 (M:200.8)	12.8	0.23
NDUBA	NADH dehydrogenase [ubiquinone] 1 beta subcomplex subunit 10	21.0	9.1	633.2 (M:633.2)	59.7	0.25	576.2 (M:576.2)	60.2	0.23
CO3	Complement C3	186.4	6.3	42.5 (M:42.5)	0.6	0.35	91.7 (M:91.7)	1.3	0.23
APOA4	Apolipoprotein A-IV	45.0	5.2	1345.7 (M:1345.7)	65.8	0.25	1168.5 (M:1168.5)	55.7	0.23
RLA2	60S acidic ribosomal protein P2	11.6	4.2	586.7 (M:586.7)	70.4	0.25	608.2 (M:608.2)	70.4	0.23
CYC	Cytochrome c, somatic	11.6	10.2	899.5 (M:899.5)	57.1	0.22	913.5 (M:913.5)	49.5	0.22
ML12B	Myosin regulatory light chain 12B	19.8	4.5	339.7 (M:339.7)	40.1	0.22	373.5 (M:373.5)	44.2	0.22
ISK3	Serine protease inhibitor Kazal-type 3	8.5	9.7	287.3 (M:287.3)	56.2	0.33	315.5 (M:315.5)	56.2	0.21
PDIA3	Protein disulfide-isomerase A3	56.6	5.8	39.6 (M:39.6)	2.2	0.35	148.8 (M:148.8)	7.3	0.21

YBOX1	Nuclease-sensitive element-binding protein 1	35.7	0.0	523.6 (M:523.6)	44.1	0.17	672.8 (M:672.8)	50.0	0.20
LY6A	Lymphocyte antigen 6A-2/6E-1	14.4	4.6	71.0 (M:71.0)	15.7	0.26	75.5 (M:75.5)	15.7	0.20
RS18	40S ribosomal protein S18	17.7	11.5	428.9 (M:428.9)	48.0	0.20	357.0 (M:357.0)	34.9	0.19
APOA1	Apolipoprotein A-I	30.6	5.4	1237.9 (M:1237.9)	66.7	0.12	1148.0 (M:1148.0)	47.7	0.15
BAP31	B-cell receptor-associated protein 31	27.9	9.3	123.9 (M:123.9)	8.2	0.26	25.5 (M:25.5)	4.1	0.12
ATIF1	ATPase inhibitor, mitochondrial	12.2	10.1	257.8 (M:257.8)	29.2	0.12	217.0 (M:217.0)	26.4	0.12

2.6. *Cell viability assessment*

All shRNA clones were obtained from National RNAi Core Facility at Academia Sinica in Taiwan. Podocytes were transfected using lipofectamine 3000 (Thermo Fisher Scientific), with or without PHB1 shRNA (TRCN0000029204), PHB2 shRNA (TRCN0000060920), or Luciferase shRNA (TRCN0000072244) for 24 h, followed by seeding into wells of 96-well plates for 24 h (5×10^3 cells per well). Following 24, 48, or 72 h of additional culture with or without cBSA (#9058, Chondrex), viable cells were estimated by measuring the conversion of 3-(4,5-dimethylthiazol-2-yl)-2,5-diphenyltetrazolium bromide (MTT) (M2128, Sigma–Aldrich) to formazan crystals.

2.7. *Western blot analysis*

Cells were lysed with lysis buffer (10 mM Tris, pH 7.5; 150 mM NaCl; 5 mM EDTA, pH 8.0; 0.1% sodium dodecyl sulfate (SDS); 1% deoxycholate; and 1% NP-40) supplemented with a protease inhibitor cocktail (Roche). Cell lysates were subjected to SDS-polyacrylamide gel electrophoresis and then transferred to polyvinylidene fluoride membranes. After blocking with 5% skim milk, the membranes were incubated with primary antibodies and subsequently with appropriate peroxidase-conjugated secondary antibodies. Information on primary antibodies, including targets, catalog numbers, dilutions, and suppliers is listed below: antibodiese specific to PHB1 (GTX101105, 1:500), PHB2 (GTX102100, 1:500), p53 (GTX100629, 1:500) were from GeneTex; antibodies specific to poly (ADP-ribose) polymerase (PARP) (#9915, 1:500) were from Cell Signaling Technology; antibodies specific to actin (MAB1501, 1:5000) was from Millipore. Blots were developed using an enhanced chemiluminescence system (Thermo Fisher Scientific). Images were cropped from different blots run under the same experimental conditions. The original blots are attached in Supplementary Fig. 1.

2.8. *RNA extraction, microarray analysis, and GO process enrichment*

The total RNA obtained from each kidney of cBSA-induced MN mice was extracted using TRIzol reagent (Invitrogen) and an RNeasy Mini kit (Qiagen) according to the manufacturer's instructions. The amount and purity of RNA were assessed as described previously [17,18]. For each group, an equal amount of total RNA extracts from each kidney were obtained ($n = 3$ in each group) for replicated runs ($n = 2$) for different groups. Target amino-allyl antisense RNA (aRNA) preparation, hybridization, scanning, and analysis were performed as previously described [17,18]. A heat map was constructed by the Multi Experiment View (MeV) software version 4.9.0 [19]. The interaction networks, as well as molecule and drug analysis, were generated by the Ingenuity Pathway Analysis (IPA) software version 01–07 (Qiagen).

2.9. *Statistical analyses*

The data were analyzed by two-way ANOVA (GraphPad Prism 8) or Student's *t*-test (Microsoft Office Excel). A P value of <0.05 was considered statistically significant.

3. Results

3.1. *PHB1 and PHB2 are upregulated in kidneys of cBSA-induced MN mice*

We first established and characterized a cBSA-induced mouse MN model. Histopathological pictures showed a diffuse thickening of the glomerular capillary walls, diffuse subepithelial fibrinoid deposits, and positive IgG immunohistochemical staining as a granular pattern of deposition along the glomerular basement membrane in MN mice, as compared to the controls (Fig. 1A). The mice with cBSA-induced MN also exhibited proteinuria (Fig. 1B).

Next, MN-related proteomic changes were determined by independent four replicate runs of label-free quantitative proteomic analyses. A total of 118 upregulated and 155 downregulated proteins after cBSA treatment were found (Supplementary Table 1). The top 20 up-/down-regulated proteins are listed in Table 1. Among the differentially expressed proteins, two mitochondrial proteins whose functions are related to proteostasis, prohibitin 1(PHB1) and prohibitin 2 (PHB2), were chosen and quantified. IHC analysis confirmed that the mouse kidneys exhibited specific histopathological changes after treatment with cBSA, and PHB1 and PHB2 were significantly upregulated in both tubular cells and the glomerulus (Fig. 1C). However, the role of PHB1 and PHB2 in cBSA-induced MN is not clear.

3.2. *Upregulation of PHB1 and PHB2 is a risk for cBSA-induced podocyte cytotoxicity*

Podocyte dysfunction, including loss of structural integrity and filter capability, is partially caused by the pathogenesis of glomerular diseases [20–22]. However, the expression of PHB under different stimuli, cell type, and cell differentiation, may have opposite effects on cell survival and apoptosis [23]. To elucidate a possible role of PHB1 and PHB2 upregulation in cBSA-induced kidney damage, the effects of cBSA on human primary podocytes were investigated. As shown in Fig. 2A, cBSA (0.1–500 μg/mL) showed a cytotoxicity to podocytes under the examined concentrations. shRNA knockdown of both PHB1 and PHB2, rescued the cBSA-induced cytotoxicity (Fig. 2A and B). In addition, both PHB1 and only PHB2 were responsible for cBSA-induced p53 upregulation and PARP upregulation and activation (Fig. 2C). These results suggest that bot PHB1 and PHB2 may predict risk for the development of cBSA-induced podocyte cytotoxicity.

3.3. *The transcriptome is regulated by cBSA in kidneys of MN mice*

To further insight into the previous findings, cBSA-induced changes in the gene expression in the kidneys were determined by a murine array. The change in cBSA-induced gene expression was determined by microarray analysis using a whole genome Mouse OneArray®. We found 72 commonly upregulated and 41 downregulated genes after cBSA treatment (Table 2), which were further selected to construct a heat map (Fig. 3A). The top up-/down-regulation-enriched association networks (based on significant differentially expressed genes) are listed in Table 3, and the top up-/down-regulation network is shown in Fig. 3B and C. The expression of the three genes [*glutamine and serine-rich 1* (*QSER1*), *chemokine* (*C-X-C motif*) *ligand 1* (*CXCL1*), and *RIKEN cDNA 2900060B14 gene* (*2900060B14RIK*)] were up-regulated at least 2.5-folds in the MN kidneys, whereas the expression of seven genes [*guanylate cyclase 1, soluble, alpha 3* (*GUCY1A3*), *chromogranin B* (*CHGB*), *WW domain-containing adapter protein with coiled-coil-like* (*LOC101056456*), *steroidogenic acute regulatory protein* (*STAR*), *hydroxy-delta-5-steroid dehydrogenase, 3 beta- and steroid delta-isomerase 1* (*HSD3B1*), *mitochondria-localized glutamic acid-rich protein* (*MGARP*), and *aldo-keto reductase family 1, member B7* (*AKR1B7*)] were down-regulated at least 2.5-folds in the MN kidneys. Although these genes are known to be expressed in the kidneys, these results are the first to document that the regulation of these genes might be involved in the

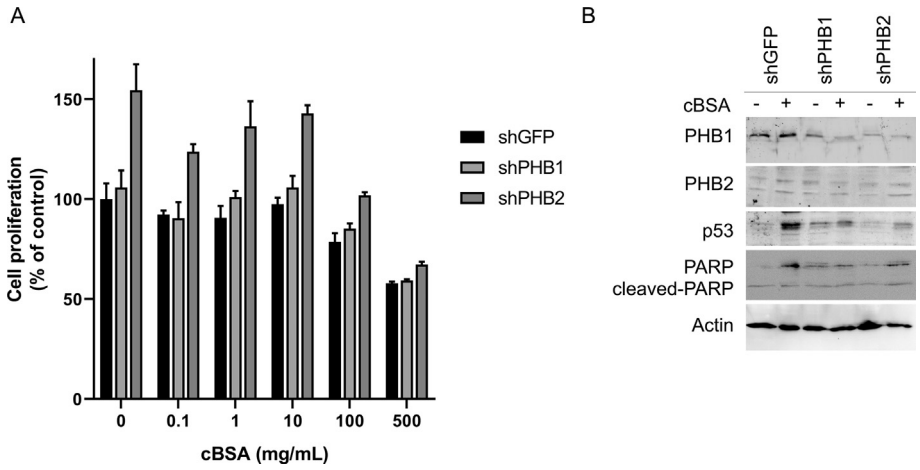

Fig. 2 – Involvement of PHB2 upregulation in cBSA-induced podocyte cytotoxicity. (A) Downregulation of PHB1 and PHB2 delays cBSA-triggered podocyte death. Podocytes were treated with cBSA (0.1–500 mg/mL) for 24 h (n = 6). The average ± SD is shown from separate experiments. ***, $p < 0.001$, **, $p < 0.01$, *, $p < 0.05$. (B) The shRNA knockdown of PHB1 and PHB2 rescued p53 upregulation and PARP upregulation/activation in response to cBSA-induced podocyte death.

Table 2 – The up-/down-regulated genes changing in response to MN development. Gene common name and description are listed. Complete dataset was shown in supplementary table 1.

RefSeq	Gene symbol	Description	Fold change (log 2 ratio) MN/Control	P value MN/Control
Upregulation				
NM_001123327.1	Qser1	glutamine and serine rich 1	NA	NA
NM_008176.3	Cxcl1	chemokine (C-X-C motif) ligand 1	3.	5.26554E-23
NR_027901.1	2900060B14Rik	RIKEN cDNA 2900060B14 gene	2.8	1.77963E-18
NM_008770.3	Cldn11	claudin 11	2.5	4.73243E-18
NM_013807.2	Plk3	polo-like kinase 3	2.5	3.28829E-15
NM_009834.2	Ccrn4l	CCR4 carbon catabolite repression 4-like (S. cerevisiae)	2.3	7.1182E-14
NM_009834.2	Ccrn4l	CCR4 carbon catabolite repression 4-like (S. cerevisiae)	2.2	3.14084E-12
NM_011414.3	Slpi	secretory leukocyte peptidase inhibitor	2.2	3.41942E-12
NM_010276.4	Gem	GTP binding protein (gene overexpressed in skeletal muscle)	1.9	7.53177E-17
NM_010444.2	Nr4a1	nuclear receptor subfamily 4, group A, member 1	1.9	3.20772E-08
NR_034045.1	Snora30	small nucleolar RNA, H/ACA box 30	1.8	4.50975E-14
NM_001164358.1,NM_001164357.1,NM_146118.3	Slc25a25	solute carrier family 25 (mitochondrial carrier, phosphate carrier), member 25	1.8	1.53833E-11
NM_026740.2	Slc46a1	solute carrier family 46, member 1	1.6	1.17382E-14
NM_011817.2	Gadd45g	growth arrest and DNA-damage-inducible 45 gamma	1.6	9.93744E-11
NM_029083.2	Ddit4	DNA-damage-inducible transcript 4	1.6	2.37554E-14
NM_001166580.1,NM_145980.2	8430408G22Rik	RIKEN cDNA 8430408G22 gene	1.5	1.24143E-13
NM_013642.3	Dusp1	dual specificity phosphatase 1	1.5	9.13322E-10
NM_001109914.1	Apold1	apolipoprotein L domain containing 1	1.4	2.84285E-07
NM_001243762.1,NM_016691.4	Clcn5	chloride channel 5	1.4	1.64728E-09
NM_010712.2	Lhx4	LIM homeobox protein 4	1.4	3.14427E-08
NM_010658.3	Mafb	v-maf musculoaponeurotic fibrosarcoma oncogene family, protein B (avian)	1.4	3.9037E-07
NM_008979.1	Ptpn22	protein tyrosine phosphatase, non-receptor type 22 (lymphoid)	1.3	6.68452E-11
NM_001159389.1,NM_177306.3	Rfx6	regulatory factor X, 6	1.3	2.92136E-08
NM_183160.3	Tmem252	transmembrane protein 252	1.3	6.13782E-06
NM_010495.2	Id1	inhibitor of DNA binding 1	1.3	8.15497E-13
NM_011084.2,NM_207683.2	Pik3c2g	phosphatidylinositol 3-kinase, C2 domain containing, gamma polypeptide	1.3	1.49897E-07
NM_172458.3	Zfp871	zinc finger protein 871	1.3	1.83766E-06
NM_153287.3	Csrnp1	cysteine-serine-rich nuclear protein 1	1.3	0.009007611
NM_053075.3	Rheb	Ras homolog enriched in brain	1.3	3.76673E-06
NM_001164096.1,NM_025298.3	Polr3e	polymerase (RNA) III (DNA directed) polypeptide E	1.3	1.49403E-11
NM_009513.2	Nrsn1	neurensin 1	1.3	9.94461E-09
NM_010755.3	Maff	v-maf musculoaponeurotic fibrosarcoma oncogene family, protein F (avian)	1.2	2.60013E-07
NM_001139509.1,NM_013613.2	Nr4a2	nuclear receptor subfamily 4, group A, member 2	1.2	1.57667E-06
NM_001081111.2	Tmf1	TATA element modulatory factor 1	1.2	5.40955E-06
NM_001113353.1,NM_001113352.1	Synj2	synaptojanin 2	1.2	9.1339E-06
NM_020507.3	Tob2	transducer of ERBB2, 2	1.2	3.64673E-07

(*continued on next page*)

Table 2 – (*continued*)

RefSeq	Gene symbol	Description	Fold change (log 2 ratio) MN/Control	P value MN/Control
NM_001110826.1,NM_181324.3, NM_007841.4	Ddx6	DEAD (Asp-Glu-Ala-Asp) box polypeptide 6	1.2	3.24208E-06
NM_134246.3	Acot3	acyl-CoA thioesterase 3	1.2	7.8905E-07
NM_010757.2	Mafk	v-maf musculoaponeurotic fibrosarcoma oncogene family, protein K (avian)	1.2	0.000208191
NM_001085410.1,NM_001040395.3	Nadkd1	NAD kinase domain containing 1	1.2	1.80878E-07
NM_144549.4	Trib1	tribbles homolog 1 (Drosophila)	1.2	3.44161E-07
NM_001113418.1,NM_011144.6	Ppara	peroxisome proliferator activated receptor alpha	1.2	1.88884E-06
NM_009964.2	Cryab	crystallin, alpha B	1.2	1.9E-05
NM_025335.3	Tmem167	transmembrane protein 167	1.1	0.000715242
NM_001159367.1,NM_011065.4	Per1	period circadian clock 1	1.1	0.006258147
NM_025404.3	Arl4d	ADP-ribosylation factor-like 4D	1.1	9.32921E-06
NM_133662.2	Ier3	immediate early response 3	1.1	1.73583E-10
NM_146630.1	Olfr123	olfactory receptor 123	1.1	6.8097E-06
NM_007856.2	Dhcr7	7-dehydrocholesterol reductase	1.1	0.000294377
NM_029305.2	1700003F12Rik	RIKEN cDNA 1700003F12 gene	1.1	2.67952E-05
NM_009621.4	Adamts1	a disintegrin-like and metallopeptidase (reprolysin type) with thrombospondin type 1 motif, 1	1.1	0.001952172
NR_015533.2	A230057D06Rik	RIKEN cDNA A230057D06 gene	1.1	2.77589E-05
NM_015747.2	Slc20a1	solute carrier family 20, member 1	1.1	4.78267E-06
NM_001025605.1	Gm527	predicted gene 527	1.1	5.98145E-07
NM_053109.3	Clec2d	C-type lectin domain family 2, member d	1.1	1.02158E-07
NM_011756.4	Zfp36	zinc finger protein 36	1.1	7.14421E-09
NM_172739.4	Grlf1	glucocorticoid receptor DNA binding factor 1	1.1	2.49466E-05
NM_145373.2	Sectm1a	secreted and transmembrane 1A	1.1	3.91122E-06
NM_010907.2	Nfkbia	nuclear factor of kappa light polypeptide gene enhancer in B cells inhibitor, alpha	1.1	4.68744E-07
NM_027708.1	Fbxo24	F-box protein 24	1.1	0.000215547
NM_010234.2	Fos	FBJ osteosarcoma oncogene	1.	3.21525E-05
NM_020601.2	Tbl1x	transducin (beta)-like 1 X-linked	1.	7.77859E-06
NM_009883.3	Cebpb	CCAAT/enhancer binding protein (C/EBP), beta	1.	0.000327993
NM_009694.3	Apobec2	apolipoprotein B mRNA editing enzyme, catalytic polypeptide 2	1.	0.000172254
NM_013840.3	Uxt	ubiquitously expressed transcript	1.	7.80088E-07
NM_010753.2	Mxd4	Max dimerization protein 4	1.	0.00078819
NM_007901.5	S1pr1	sphingosine-1-phosphate receptor 1	1.	0.000556851
NM_139309.4	Fktn	fukutin	1.	0.000135171
NM_015786.2	Hist1h1c	histone cluster 1, H1c	1.	9.94486E-07
NM_001032414.1, NM_001032413.1,NM_152799.2, NM_028460.2	Pear1	platelet endothelial aggregation receptor 1	1.	0.005645171
NM_172873.3	Cdcp2	CUB domain containing protein 2	1.	0.001820074
XR_168586.1, XR_168782.1	Gm10755	predicted gene 10755	1.	0.000155765

Downregulation				
NM_021896.5	Gucy1a3	guanylate cyclase 1, soluble, alpha 3	NA	NA
NM_007694.4	Chgb	chromogranin B	NA	NA
XM_003946015.1, XM_003946014.1,XM_003946013.1 ,XM_003946012.1,XM_003946011.1 ,XM_003946010.1	LOC101056456	WW domain-containing adapter protein with coiled-coil-like	NA	NA
NM_011485.4	Star	steroidogenic acute regulatory protein	NA	NA
NM_008293.3	Hsd3b1	hydroxy-delta-5-steroid dehydrogenase, 3 beta- and steroid delta-isomerase 1	−5.9	1.90603E-39
NM_026358.3, NR_028121.1	Mgarp	mitochondria localized glutamic acid rich protein	−4.3	1.39302E-22
NM_009731.2	Akr1b7	aldo-keto reductase family 1, member B7	−3.	1.61605E-18
NM_153062.2, NM_001242427.1	Slc37a1	solute carrier family 37 (glycerol-3-phosphate transporter), member 1	−2.3	1.07528E-12
NM_013697.5	Ttr	transthyretin	−2.	1.29844E-17
NR_002865.2	Rnu11	U11 small nuclear RNA	−2.	3.69595E-09
NM_011399.3	Slc25a17	solute carrier family 25 (mitochondrial carrier, peroxisomal membrane protein), member 17	−1.9	4.35113E-21
NM_013474.2	Apoa2	apolipoprotein A-II	−1.8	1.46536E-17
NM_023456.2	Npy	neuropeptide Y	−1.8	2.3199E-15
NM_020567.2	Gmnn	geminin	−1.7	2.08837E-11
NM_011254.5	Rbp1	retinol binding protein 1, cellular	−1.7	1.53166E-13
NM_010479.2	Hspa1a	heat shock protein 1A	−1.7	2.40272E-10
NM_009654.3	Alb	albumin	−1.7	4.95334E-07
NR_046233.1	Rn45s	45S pre-ribosomal RNA	−1.6	9.21288E-13
NM_001012323.1|XM_003945754.1	Mup20|LOC101055795	major urinary protein 20|major urinary protein 5-like	−1.6	3.86299E-12
NM_007751.3	Cox8b	cytochrome c oxidase subunit VIIIb	−1.6	3.09785E-14
NM_001102446.1,NM_009653.3	Alas2	aminolevulinic acid synthase 2, erythroid	−1.6	4.49199E-06
NM_007702.2	Cidea	cell death-inducing DNA fragmentation factor, alpha subunit-like effector A	−1.5	1.60602E-08
NM_008917.3	Ppt1	palmitoyl-protein thioesterase 1	−1.5	0.001784114
NM_008220.4| NM_016956.2	Hbb-b1|Hbb-b2	hemoglobin, beta adult major chain|hemoglobin, beta adult minor chain	−1.5	1.36229E-16
NM_009463.3	Ucp1	uncoupling protein 1 (mitochondrial, proton carrier)	−1.5	3.31087E-11
NR_029805.1	Mir211	microRNA 211	−1.4	3.18911E-13
NM_026998.3	Snx6	sorting nexin 6	−1.4	1.91533E-09
NM_024283.3	1500015O10Rik	RIKEN cDNA 1500015O10 gene	−1.4	8.77389E-06
NM_016669.1	Crym	crystallin, mu	−1.3	1.38972E-10
NM_053188.2	Srd5a2	steroid 5 alpha-reductase 2	−1.3	4.47489E-07
NM_010253.3	Gal	galanin	−1.3	2.41957E-07
XM_003945873.1	LOC101056505	uncharacterized LOC101056505	−1.2	1.90126E-05
NR_004414.1	Rnu2-10	U2 small nuclear RNA 10	−1.2	1.76133E-06
NM_009377.1	Th	tyrosine hydroxylase	−1.2	0.000267084
NM_010478.2	Hspa1b	heat shock protein 1B	−1.2	3.74997E-08
NM_001029842.1,NM_134038.2	Slc16a6	solute carrier family 16 (monocarboxylic acid transporters), member 6	−1.1	1.38544E-06

(*continued on next page*)

Table 2 – (continued)

RefSeq	Gene symbol	Description	Fold change (log 2 ratio) MN/Control	P value MN/Control
NM_145530.2	Rhov	ras homolog gene family, member V	−1.1	1.84464E-06
NM_026716.3	Sycn	syncollin	−1.1	8.64018E-08
NM_008597.3	Mgp	matrix Gla protein	−1.	1.56343E-07
NM_009692.3	Apoa1	apolipoprotein A-I	−1.	2.41029E-06
NM_001102407.1,NM_025875.2	Rbm8a	RNA binding motif protein 8a	−1.	8.51165E-05

development of MN. The changes in gene expression of PHB1 and PHB2 detected by arrays were not significantly altered, which indicated that the upregulation of PHB1 and PHB2 protein levels might have resulted from the prevention of protein degradation. Networks generated by Ingenuity Pathway Analysis software identified nodes, including upregulation of *NR4A1*, *FOS*, *AP1*, *PPARA*, *CEBPB*, and *NFKBIA*, and downregulation of *HDL* and *APOA2*, which might help to explain the functional mechanisms of cBSA-induced MN development. Taken together, these results demonstrate that cBSA-induced MN may result from the downregulation of cellular catabolic processes and result in proteostasis, which may provide information on differential mRNA profiles for cBSA-induced nephrotoxicity.

4. Discussion

Here we used proteomic expression analysis to identify differentially expressed proteins associated with the development of cBSA-induced MN in a mouse model. Two proteins, PHB1 and PHB2, were upregulated in cBSA-induced MN kidneys in mice, which may play a role in promoting podocyte death. Modulation of expression of PHB1, especially PHB2, may help in rescuing cBSA-induced podocyte death through tumor suppressor p53.

The precise mechanism by which antigens, such as cBSA that is found in food, promote MN, remains to be elucidated. Here, although we did not differentiate which component of the renal cortex contributed to RNA or protein expression, we found that both glomerular and tubular responses contributed to the organ response in MN, as revealed by microarray and label-free quantitative proteomics analyses. PHBs are evolutionarily conserved genes that are ubiquitously expressed in the nucleus, mitochondria, and cytosol, and are also associated with some cell membrane receptors [24]. Dysfunctions of PHBs are known to be associated with aging [25], neurodegenerative diseases [26], and metabolic diseases [27]. Global knockdown of PHBs leads to embryonic lethality in mice [25,28]. In podocytes, PHB1 and PHB2 work as protein scaffolds and as key checkpoints for maintaining cell survival and normal cellular structure [29]. This study emphasizes that upregulation of PHB1 and PHB2 may be new targets for rapid screening of MN, but further evaluation with clinical samples is required.

Limitations of this study include a lack of comparison with non-MN types of kidney diseases, in part due to underdevelopment of reliable models and differences in species. Data obtained using high-throughput techniques are generally required to be validated by other methods. The identified peptide in LC-MS/MS can be validated through determining aberrant expression through use of immunohistochemistry analysis in organs. Use of established resources, including databases, may also provide opportunities for further understanding the pathological mechanisms of MN, and will also provide insights into screening and development of new drugs for treatment.

In summary, here we investigated protein expression in a cBSA-induced MN mouse model using a high-throughput method. Our findings suggest that PHB1 and PHB2 may be

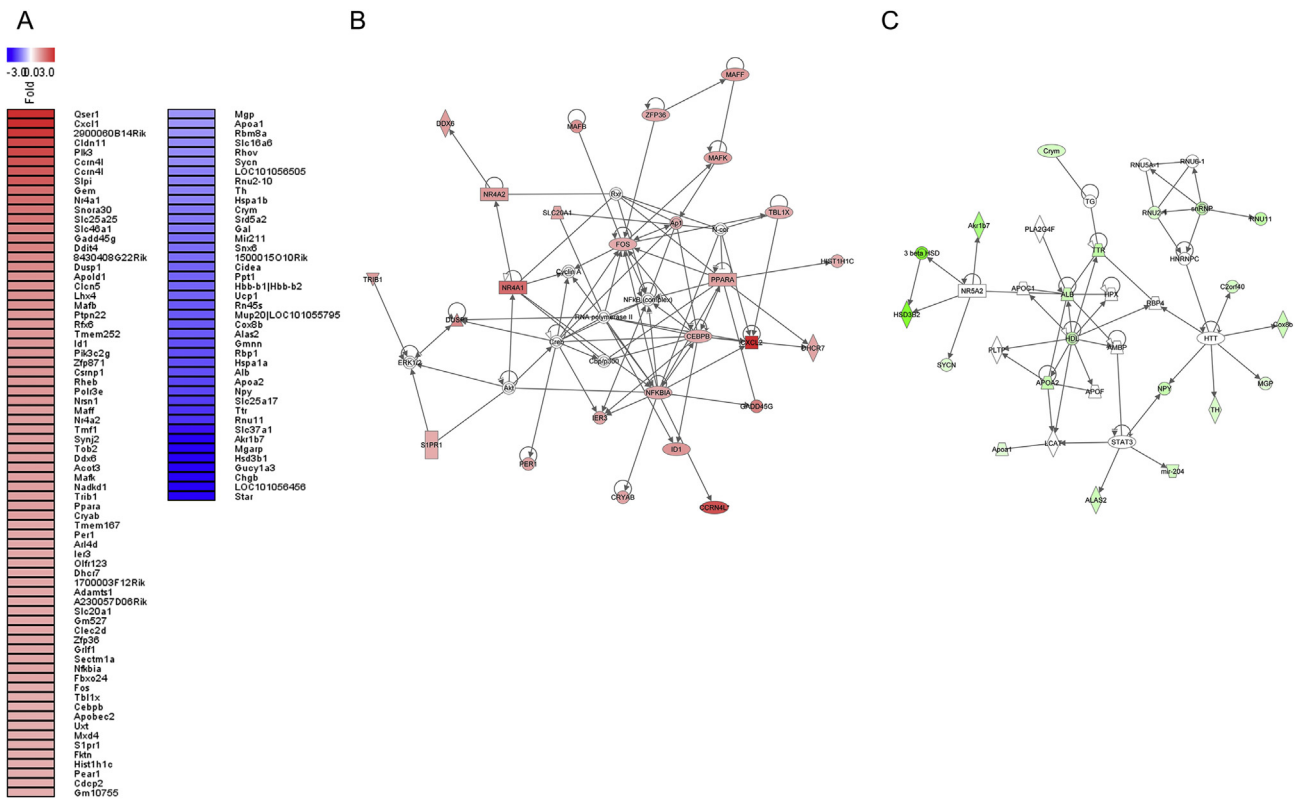

Fig. 3 – Transcription expression profiles of kidney tissues from mice with or without MN. (A) Heat map representing cationic bovine serum albumin (cBSA)-regulated genes (72 upregulated, red; 41 downregulated, blue) obtained from kidney tissues from mice treated with or without cBSA. (B) Networks of the top common cBSA up- and down-regulated genes in kidneys of mice with or without MN are shown using Ingenuity pathway analysis. The colors of the nodes show the fold changes of differentially expressed genes between cBSA-treated and control cells (red, upregulated genes; green, downregulated genes). Functional connections are indicated with arrows.

Table 3 – The top up-/down-regulation enriched association networks.

ID	Associated Network Functions	Score
Upregulation		
1	Gene Expression, Connective Tissue Disorders, Immunological Disease	60
2	Nucleic Acid Metabolism, Lipid Metabolism, Small Molecule Biochemistry	24
3	Cellular Development, Cellular Growth and Proliferation, Lymphoid Tissue Structure and Development	18
4	Cell Cycle, Cancer, Endocrine System Disorders	16
5	Cell Cycle, Cell Morphology, Cellular Assembly and Organization	2
Downregulation		
1	Lipid Metabolism, Molecular Transport, Small Molecule Biochemistry	41
2	Dermatological Diseases and Conditions, Nutritional Disease, Cancer	33
3	Cell Signaling, Cellular Development, Cellular Growth and Proliferation	2

new potential targets for development of diagnostic and/or therapeutics for MN, however, additional studies are necessary to determine the causal relationship between the upregulation of PHB1 and PHB2 and the development of MN.

Declaration of Competing Interest

The authors declare that they have no conflict of interest.

Acknowledgments

We thank the National RNAi Core Facility at Academia Sinica in Taiwan for providing shRNA reagents and related services, and the Taiwan Animal Consortium (MOST 107-2319-B-001-002) – Taiwan Mouse Clinic, which was funded by the Ministry of Science and Technology (MOST) of Taiwan, for technical support in all IHC slide scanning. This study was supported by MOST of Taiwan (NSC 100-2314-B-039-031-, MOST 107-2320-B-

039-032-MY3), China Medical University (CMU103-S-20) and Health and welfare surcharge of tobacco products, and China Medical University Hospital Cancer Research Center of Excellence (MOHW108-TDU-B-212-124024, Taiwan).

Appendix A. Supplementary data

Supplementary data to this article can be found online at https://doi.org/10.1016/j.jfda.2019.09.003.

REFERENCES

[1] Hung PH, Shen CH, Tsai HB, Hsiao CY, Chiang PC, Guo HR, et al. Urothelial carcinoma in patients with advanced kidney disease: a 12-year retrospective cohort survey. Am J Med Sci 2011;342:148–52.
[2] Glassock RJ. The pathogenesis of idiopathic membranous nephropathy: a 50-year odyssey. Am J Kidney Dis : Off J Natl Kidney Found 2010;56:157–67.
[3] Debiec H, Lefeu F, Kemper MJ, Niaudet P, Deschenes G, Remuzzi G, et al. Early-childhood membranous nephropathy due to cationic bovine serum albumin. N Engl J Med 2011;364:2101–10.
[4] Debiec H, Guigonis V, Mougenot B, Decobert F, Haymann JP, Bensman A, et al. Antenatal membranous glomerulonephritis due to anti-neutral endopeptidase antibodies. N Engl J Med 2002;346:2053–60 [In eng].
[5] Stahl R, Hoxha E, Fechner K. PLA2R autoantibodies and recurrent membranous nephropathy after transplantation. N Engl J Med 2010;363:496–8 [In eng].
[6] Hoxha E, Thiele I, Zahner G, Panzer U, Harendza S, Stahl RA. Phospholipase A2 receptor autoantibodies and clinical outcome in patients with primary membranous nephropathy. J Am Soc Nephrol : JASN 2014;25:1357–66 [In eng].
[7] Hoxha E, Harendza S, Pinnschmidt H, Panzer U, Stahl RA. M-type phospholipase A2 receptor autoantibodies and renal function in patients with primary membranous nephropathy. Clin J Am Soc Nephrol : CJASN 2014;9:1883–90 [In eng].
[8] Kanigicherla D, Gummadova J, McKenzie EA, Roberts SA, Harris S, Nikam M, et al. Anti-PLA2R antibodies measured by ELISA predict long-term outcome in a prevalent population of patients with idiopathic membranous nephropathy. Kidney Int 2013;83:940–8 [In eng].
[9] Tomas NM, Hoxha E, Reinicke AT, Fester L, Helmchen U, Gerth J, et al. Autoantibodies against thrombospondin type 1 domain-containing 7A induce membranous nephropathy. J Clin Investig 2016;126:2519–32 [In eng].
[10] Godel M, Grahammer F, Huber TB. Thrombospondin type-1 domain-containing 7A in idiopathic membranous nephropathy. N Engl J Med 2015;372:1073 [In eng].
[11] Meyer-Schwesinger C, Lambeau G, Stahl RA. Thrombospondin type-1 domain-containing 7A in idiopathic membranous nephropathy. N Engl J Med 2015;372:1074–5 [In eng].
[12] Tomas NM, Beck Jr LH, Meyer-Schwesinger C, Seitz-Polski B, Ma H, Zahner G, et al. Thrombospondin type-1 domain-containing 7A in idiopathic membranous nephropathy. N Engl J Med 2014;371:2277–87 [In eng].
[13] Chen JS, Chen A, Chang LC, Chang WS, Lee HS, Lin SH, et al. Mouse model of membranous nephropathy induced by cationic bovine serum albumin: antigen dose-response relations and strain differences. Nephrol Dial Transplant 2004;19:2721–8.
[14] Borza DB, Zhang JJ, Beck Jr LH, Meyer-Schwesinger C, Luo W. Mouse models of membranous nephropathy: the road less travelled by Afr J Clin Exp Immunol 2013;2:135–45.
[15] Ronco P, Debiec H. Pathogenesis of membranous nephropathy: recent advances and future challenges. Nat Rev Nephrol 2012;8:203–13.
[16] Chen YH, Chen CJ, Yeh S, Lin YN, Wu YC, Hsieh WT, et al. Urethral dysfunction in female mice with estrogen receptor beta deficiency. PLoS One 2014;9:e109058 [In eng].
[17] Liu YH, Weng YP, Lin HY, Tang SW, Chen CJ, Liang CJ, et al. Aqueous extract of Polygonum bistorta modulates proteostasis by ROS-induced ER stress in human hepatoma cells. Sci Rep 2017;7:41437.
[18] Liu YH, Weng YP, Tsai HY, Chen CJ, Lee DY, Hsieh CL, et al. Aqueous extracts of Paeonia suffruticosa modulates mitochondrial proteostasis by reactive oxygen species-induced endoplasmic reticulum stress in pancreatic cancer cells. Phytomedicine 2018;46:184–92.
[19] Saeed AI, Sharov V, White J, Li J, Liang W, Bhagabati N, et al. TM4: a free, open-source system for microarray data management and analysis. Biotechniques 2003;34:374–8.
[20] Reddy GR, Kotlyarevska K, Ransom RF, Menon RK. The podocyte and diabetes mellitus: is the podocyte the key to the origins of diabetic nephropathy? Curr Opin Nephrol Hypertens 2008;17:32–6 [In eng].
[21] Marshall SM. The podocyte: a potential therapeutic target in diabetic nephropathy? Curr Pharmaceut Des 2007;13:2713–20 [In eng].
[22] Li JJ, Kwak SJ, Jung DS, Kim JJ, Yoo TH, Ryu DR, et al. Podocyte biology in diabetic nephropathy. Kidney Int Suppl 2007:S36–42 [In eng].
[23] Peng YT, Chen P, Ouyang RY, Song L. Multifaceted role of prohibitin in cell survival and apoptosis. Apoptosis 2015;20:1135–49.
[24] Thuaud F, Ribeiro N, Nebigil CG, Desaubry L. Prohibitin ligands in cell death and survival: mode of action and therapeutic potential. Chem Biol 2013;20:316–31 [In eng].
[25] Artal-Sanz M, Tavernarakis N. Prohibitin couples diapause signalling to mitochondrial metabolism during ageing in C. elegans. Nature 2009;461:793–7 [In eng].
[26] Dutta D, Ali N, Banerjee E, Singh R, Naskar A, Paidi RK, et al. Low levels of prohibitin in substantia nigra makes dopaminergic neurons vulnerable in Parkinson's disease. Mol Neurobiol 2018;55:804–21 [In eng].
[27] Ising C, Koehler S, Brahler S, Merkwirth C, Hohne M, Baris OR, et al. Inhibition of insulin/IGF-1 receptor signaling protects from mitochondria-mediated kidney failure. EMBO Mol Med 2015;7:275–87 [In eng].
[28] Park SE, Xu J, Frolova A, Liao L, O'Malley BW, Katzenellenbogen BS. Genetic deletion of the repressor of estrogen receptor activity (REA) enhances the response to estrogen in target tissues in vivo. Mol Cell Biol 2005;25:1989–99 [In eng].
[29] Signorile A, Sgaramella G, Bellomo F, De Rasmo D. Prohibitins: a critical role in mitochondrial functions and implication in diseases. Cells 2019;8 [In eng].